

SSY345 Smartphone Project

Yongzhao Chen(yongzhao@chalmers.se)

May 30, 2023

1 Q1: Choices of input and output

1.1 As input

Pros of selecting $u_k = w_k$ (using angular velocities as inputs):

1. Accuracy: Gyroscope measurements of angular velocities are typically more accurate and less prone to noise compared to other sensor measurements. Using them as inputs can improve the accuracy of the estimation process.

2. Reduced computational complexity: Using angular velocities as inputs reduces the dimensionality of the state vector, simplifying the estimation algorithm and reducing computational requirements. This leads to faster execution and lower resource consumption.

Cons of selecting $u_k = w_k$:

1. Susceptibility to gyro drift: Gyroscopes can experience drift over time, leading to errors in the estimated orientation. Extended operation without external reference or correction can cause gradual deviation from the true orientation.

2. Lack of absolute reference: Using angular velocities as inputs does not provide an absolute reference for the system's orientation. The estimated orientation may drift over time, especially without external measurements or references to correct cumulative errors.

In fact, in subsequent experiments, it was observed that the gyroscope exhibits high accuracy and is subjected to minimal disturbances, making it well-suited for use as an input.

1.2 As state

Including angular velocities in the state vector is beneficial in the following situations:

1. Dynamic Systems: If the system being modeled has complex dynamics that cannot be accurately captured solely by measurements, including angular velocities as state variables provides a more comprehensive representation of the system's behavior.

2. Noisy Measurements: If the measurements of angular velocities are noisy or subject to significant disturbances, including them as state variables helps mitigate the impact of measurement uncertainties.

3. Biased Measurements: When measurements of angular velocities suffer from biases, incorporating them as state variables and estimating the biases allows the estimation algorithm to compensate for these biases and provide more accurate results.

2 Task 2

In this task, I placed the phone on the table without any touch or movement.

When the phone is placed flat on a table, the accelerometer should read the gravitational acceleration on the Z-axis, while the readings on the X and Y axes should be zero. The readings of the gyroscope should be zero in all three directions, while the magnetometer readings should reflect the magnetic field strength of the phone's current position.

Since the last moment I touched the screen to stop stream, so in calculation I threw the last 0.1 second data away to avoid disturbances.

2.1 True state

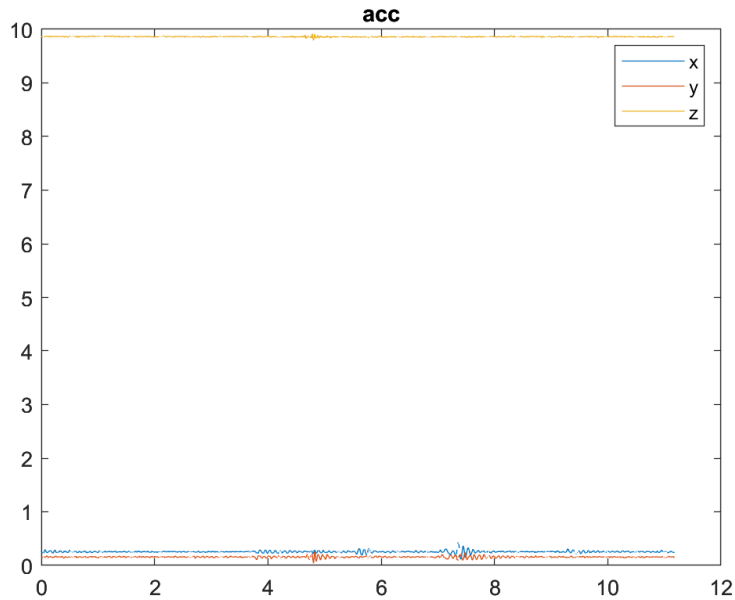


Figure 1: Accelerometers

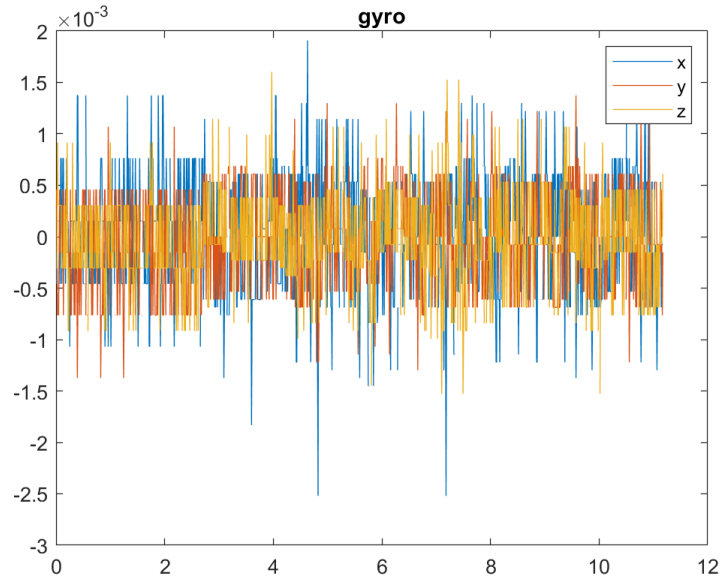


Figure 2: Gyroscope

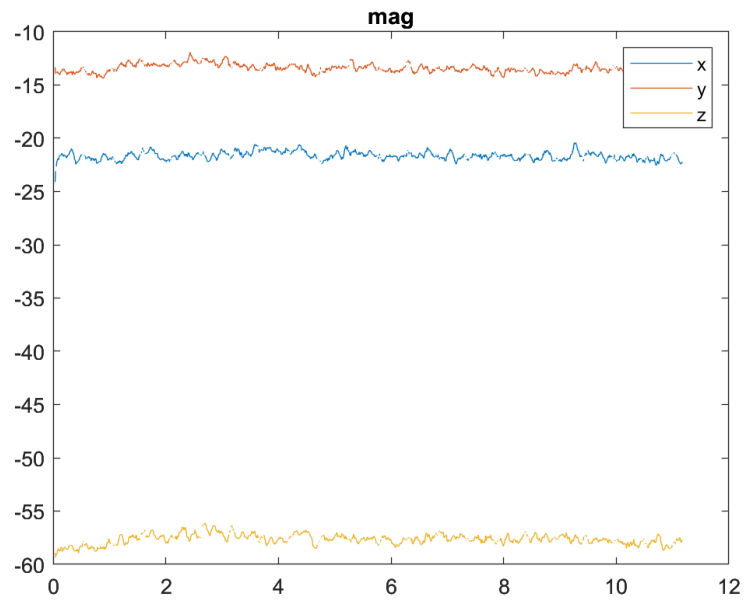


Figure 3: Magnetometers

Through observation of the sensor plots, it is evident that when the phone is placed flat on a table, the readings from all three sensors demonstrate a consistent

and stable trend without notable disturbances.

2.2 Mean and covariance and histograms

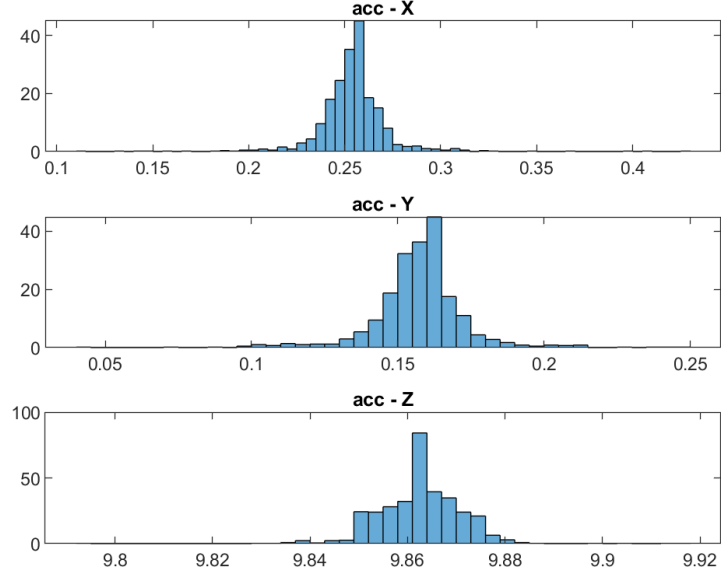


Figure 4: Histograms for accelerometers

The mean of acc -X is 0.254171 , the covariance of acc -X is 0.019724

The mean of acc -Y is 0.157052 , the covariance of acc -Y is 0.016096

The mean of acc -Z is 9.862452 , the covariance of acc -Z is 0.008445

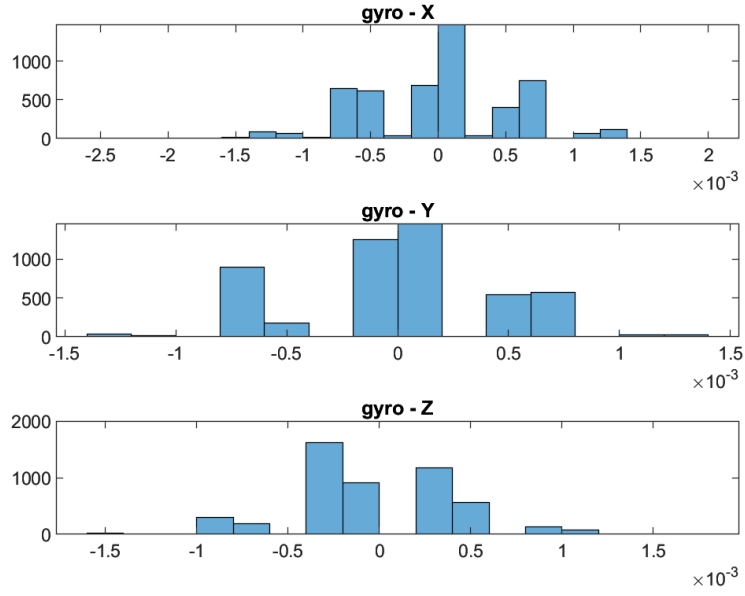


Figure 5: Histograms for gyroscope

The mean of gyro -X is 0.000014 , the covariance of gyro -X is 0.000554

The mean of gyro -Y is -0.000031 , the covariance of gyro -Y is 0.000449

The mean of gyro -Z is -0.000025 , the covariance of gyro -Z is 0.000453

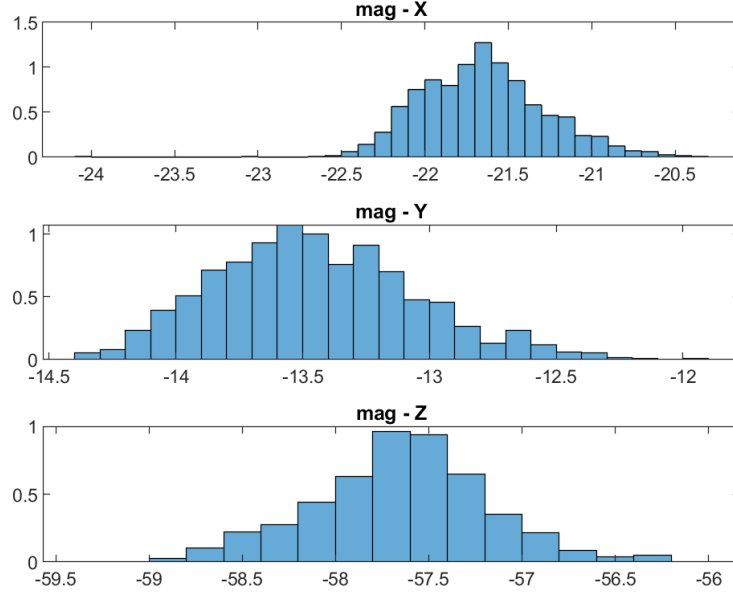


Figure 6: Histograms for magnetometers

The mean of mag -X is -21.648532 , the covariance of mag -X is 0.377973

The mean of mag -Y is -13.445163 , the covariance of mag -Y is 0.401212

The mean of mag -Z is -57.647071 , the covariance of mag -Z is 0.477309

The histogram of the accelerometer (acc) displays a distribution closely resembling a Gaussian shape, with a slight offset around the mean. This offset can likely be attributed to initial calibration errors during sensor measurements. Considering the protrusion of the rear camera on my phone, it is plausible that the mean offset of the accelerometer is influenced by the components of gravitational acceleration along the corresponding coordinate axes. As the phone is unlikely to be placed on a table for future measurements, this error can be mitigated. Therefore, it is reasonable to treat the accelerometer noise as Gaussian noise.

The histogram of the gyroscope (gyro) does not precisely align with a Gaussian distribution. This discrepancy may be due to the extremely small measurement errors of the gyroscope. Even if there are some offsets, the histogram shape may not exhibit a pronounced Gaussian distribution due to the minimal presence of noise. The noise in the gyroscope is exceptionally small, rendering it highly reliable. Therefore, during the subsequent tuning process, it can be assumed to have negligible measurement model noise and set to zero.

The histogram of the magnetometer (mag) exhibits a shape resembling a Gaussian distribution, albeit with an overall offset. This offset could be influenced by environmental noise in the magnetic field or biases in the magnetometer. To ensure accurate measurements, it is recommended to calibrate the magnetometer based on the current environment before each use, taking into account the specific requirements of the subsequent content.

In the subsequent experiments, I placed the mobile phone on a roll of paper to ensure that the mobile phone's XY plane was parallel to the table as much as possible. This also extended the measurement time. Therefore, new measurement values were used in the last few tasks, but they were all based on the `calculation` function.

3 Design the EKF time update step

3.1 Task 3

To derive a discretized model from the continuous time model in equation (5), we can solve the differential equation and use the relation $\exp(A) \approx I + A$ to obtain the discretized form. Here's the derivation:

The continuous time model is :

$$\dot{q}(t) = \frac{1}{2}S(w_{k-1} + v_{k-1})q(t) \quad (1)$$

Use the relation $\exp(At) \approx I + At$ to solve ODE:

$$q(t + T) = \exp\left(\frac{1}{2}S(w_{k-1} + v_{k-1})T\right) \cdot q(t) = \left[\mathbf{I} + \frac{T}{2}S(w_{k-1} + v_{k-1})\right] \cdot q(t) \quad (2)$$

T is the sample time interval. And the form can be translated into a discretized style:

$$\begin{aligned} q_k &= \mathbf{I} \cdot q_{k-1} + \frac{T}{2}S(w_{k-1} + v_{k-1}) \cdot q_{k-1} \\ &= \left(\mathbf{I} + \frac{T}{2}S(w_{k-1})\right) \cdot q_{k-1} + \frac{T}{2}S(v_{k-1}) \cdot q_{k-1} \end{aligned} \quad (3)$$

So we get:

$$\begin{aligned} F(\omega_{k-1}) &= \mathbf{I} + \frac{T}{2} \cdot S(\omega_{k-1}) \\ G(\hat{q}_{k-1}) &= \frac{T}{2} \cdot S(\hat{q}_{k-1}) \end{aligned} \tag{4}$$

3.1.1 Reason for Discretize

In the EKF, the prediction step involves propagating the state estimate and covariance from the previous time step to the current time step. This propagation is typically done using the continuous-time dynamic model, which can be linearized around the current state estimate. However, linearizing the model can introduce errors, especially for highly nonlinear systems.

To address this issue, the discretized model derived using the approximation techniques provides an alternative approach for the prediction step in the EKF. By discretizing the continuous-time dynamic model, we can directly apply it in the discrete-time domain without the need for linearization.

3.2 Task 4

If there are angular velocities, update the estimate and covariance as motion model, in function `tu_qw`.

Once v_k is missing, use the same consideration as in homework 2, skip the update for the current time, and keep the state and covariance value as the latest update value.

3.3 Task 5

In the function `Task5_filterTemple`, I utilized the `tu_qw` and `mu_normalizeQ` functions for the gyroscope sensor.

As observed and analyzed previously, the gyroscope provides accurate angular velocities but cannot obtain the absolute orientation.

To address this, I established the initial flat state by starting with the phone facing left and standing on its left edge. However, during the process, it consistently exhibits an offset compared to the orientation measurement, which is displayed as 'Google'.

Additionally, the gyroscope is prone to drifting due to this bias. To demonstrate this behavior, I conducted a procedure where I placed the phone on a table, shook it for a period of time, and then returned it to its original position. I repeated this procedure twice, and the resulting drift process is clearly depicted in Figure 7.

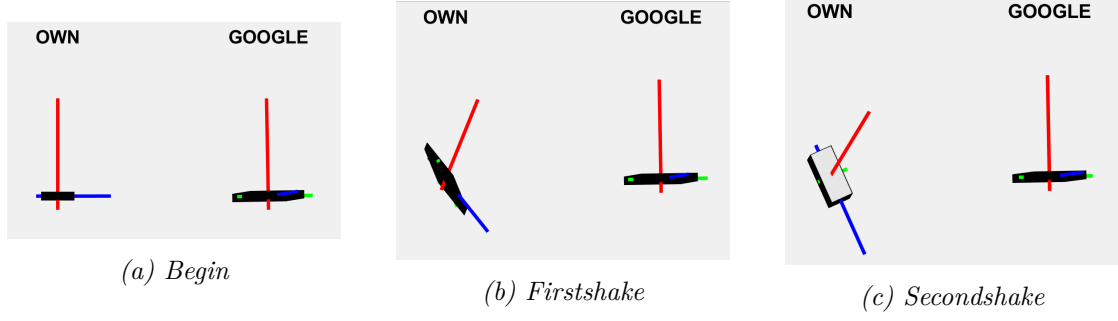


Figure 7: Drift Process

4 Accelerometer

4.1 Task 6

The question here is similar to homework3 , the pre-function about calculating $[Hx; hx]$.

The measurement model is $y_k^a = Q^T(q_k)(g^0 + f_k^a) + e_k^a$, in which we assume $f_k^a = 0$. Then the $hx = Q^T(q_k) \cdot g^0$, $Hx = \frac{\partial hx}{\partial q_k} = \frac{dQ(q_k)}{dq} \cdot g^0$. In addition, the updating process is :

$$\begin{aligned}\hat{\mathbf{x}}_{k|k} &= \hat{\mathbf{x}}_{k|k-1} + \mathbf{K}_k \mathbf{v}_k \\ \mathbf{P}_{k|k} &= \mathbf{P}_{k|k-1} - \mathbf{K}_k \mathbf{S}_k \mathbf{K}_k^T \\ \text{where} \\ Q &= Q(q(x)), \mathbf{h} = Q'(g)^0; \\ [Q0, \quad Q1, \quad Q2, \quad Q3] &= dQ(q)dx; \\ \mathbf{H} &= [Q0'(g)^0 \quad Q1'(g)^0 \quad Q2'(g)^0 \quad Q3'(g)^0]; \\ \mathbf{K}_k &= \mathbf{P}_{k|k-1} \mathbf{H}_k^T \mathbf{S}_k^{-1} \\ \mathbf{v}_k &= \mathbf{y}_k - \mathbf{H}_k \hat{\mathbf{x}}_{k|k-1} \\ \mathbf{S}_k &= \mathbf{H}_k \mathbf{P}_{k|k-1} \mathbf{H}_k^T + \mathbf{R}_k\end{aligned}$$

The $\hat{\mathbf{x}}_{k|k}$ and $\mathbf{P}_{k|k}$ above are the return value of the function `mu_g`.

4.2 Task 7

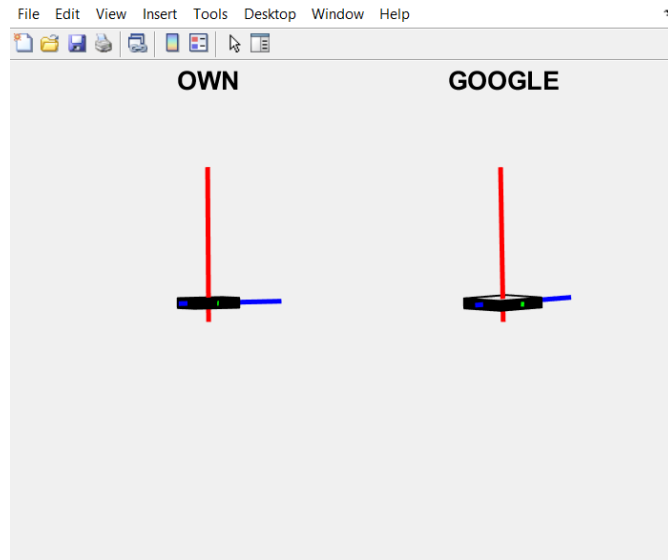


Figure 8: Task 7 Start figure

Move the phone right and left at a slow speed repeatedly:

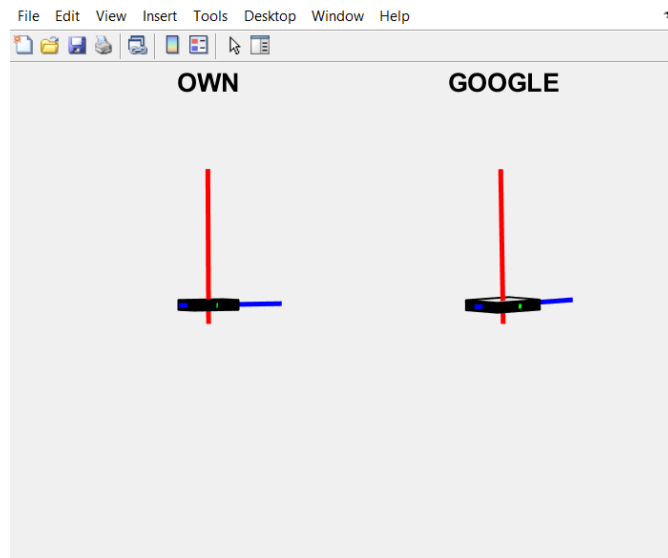


Figure 9: Right left move

Flip the phone to the right side and lay it down repeatedly:

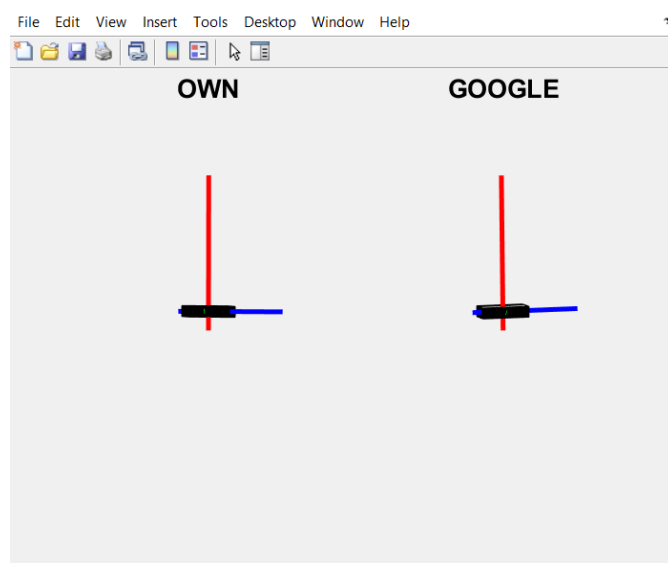


Figure 10: Flip right

Fastly flip it forward and back:

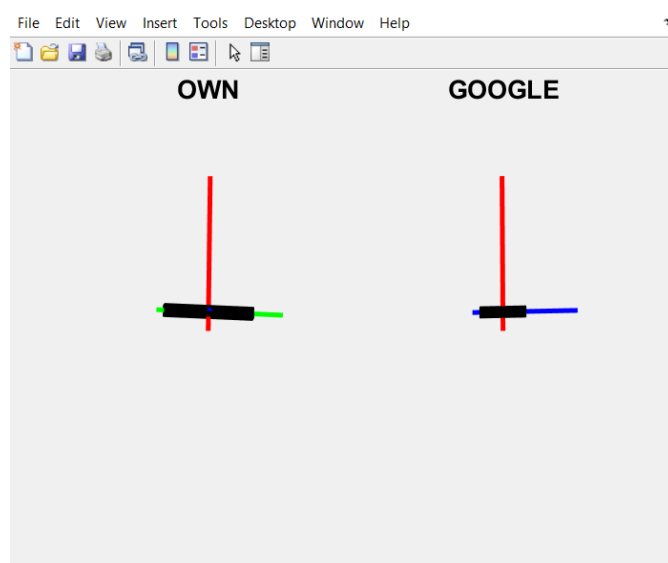


Figure 11: Flip forward

Fastly rotate it around \mathbf{y} :

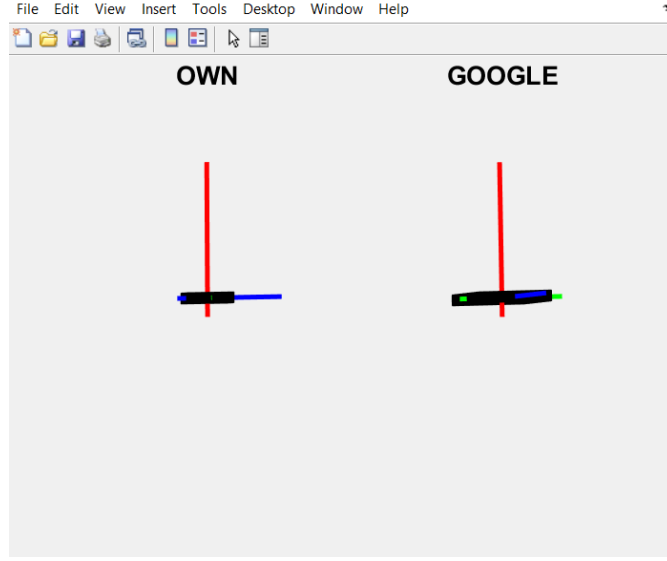


Figure 12: Rotate around y

Fastly go to right:

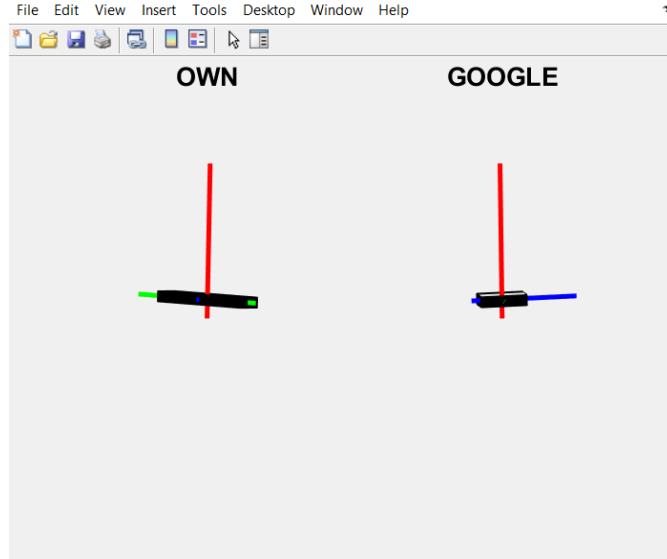


Figure 13: Fastly go right

During the testing process, we have observed that if the phone does not experience significant acceleration, its own orientation estimate will not drift significantly. However, when the phone undergoes a substantial acceleration that cannot be ignored, such as the force f_k^a , the estimated posture will exhibit significant drift.

4.3 Task 8

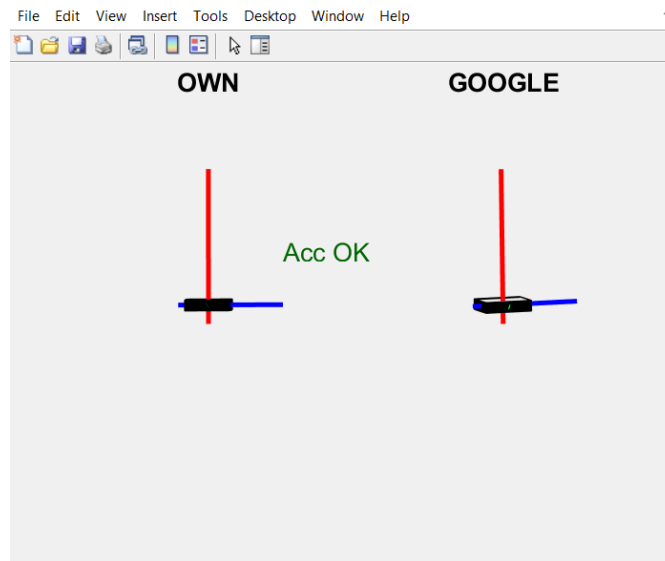


Figure 14: 20% range - begin

Set outlier range as 20%:

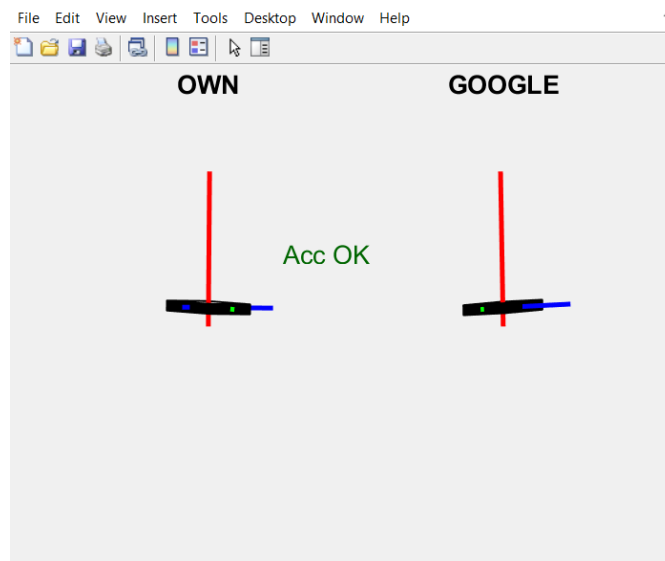


Figure 15: 20% range - end

We find that 20% outlier range is too big that cannot fix the drift, so try to set the range as 10%:

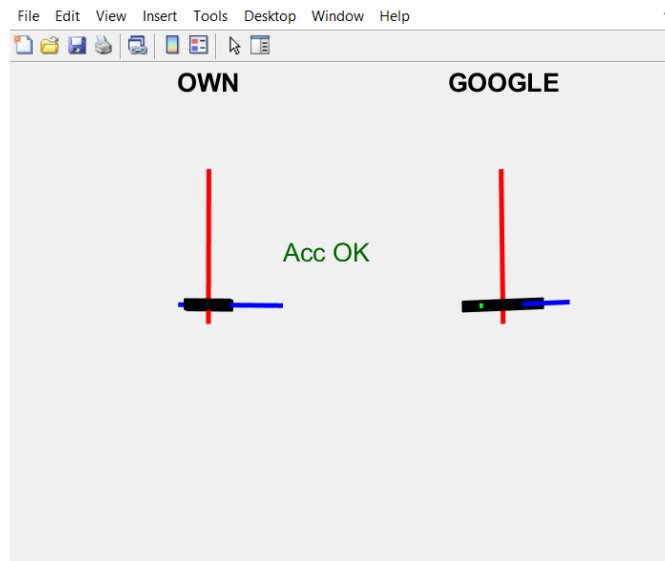


Figure 16: 10% range - begin

After performing rapid back-and-forth shaking of the phone, it appears that the previous drift issue has been mostly resolved.

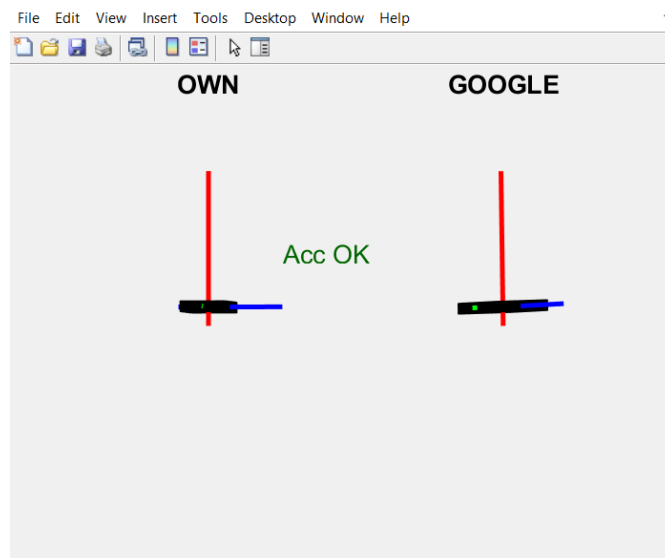


Figure 17: 10% range - end

But after some violent shake, the result still says it is not good:

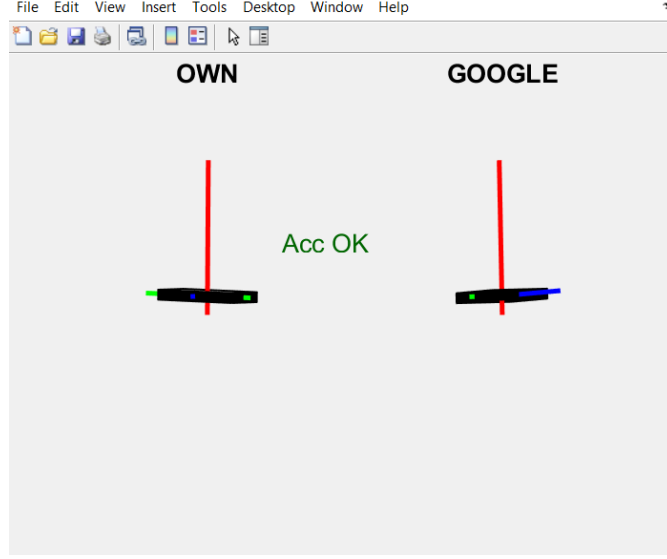


Figure 18: capital

In conclusion, after updating the outlier detection and implementing a rejection threshold, we have observed that the current attitude estimation is able to mitigate the drift issue observed in previous experiments, as long as the acceleration is not excessively high. This outcome aligns with our expectations, as updates falling outside the acceptable range are rejected.

However, we have also noticed that even with the implementation of this simple rejection algorithm, there is still some deviation in the attitude estimation after intense and multi-directional shaking acceleration. This can be attributed to the fact that the orientation estimation algorithm involves integrating accelerometer measurements over time to estimate orientation. Integration introduces cumulative errors, and even small inaccuracies in the accelerometer measurements can result in significant drift over time. Outlier rejection alone may not be sufficient to compensate for these integration errors and maintain accurate orientation estimates.

5 An EKF update using magnetometer measurements

5.1 Task 9

For this segment, I have undertaken a fresh measurement of the magnetic parameters to recalibrate the magnetometer's offset.

The theory of the EKF filter is the same as the accelerometer part, and the function `mu_m` is exactly modified from `mu_g`. So I do not derive the kalman filter theory here again.

5.2 Task 10

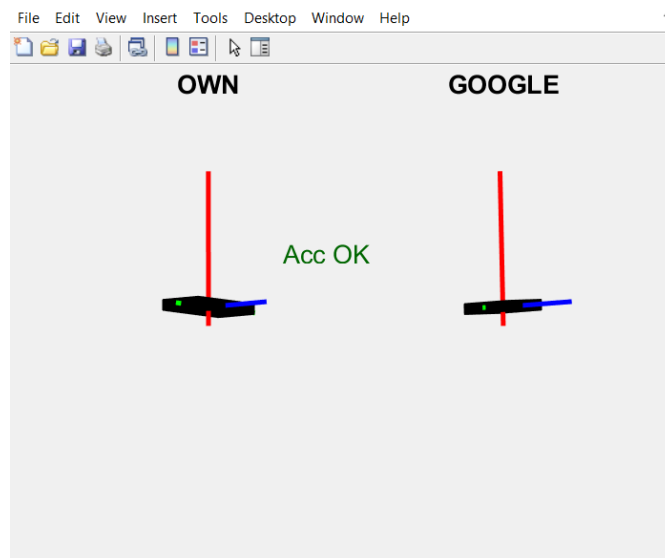


Figure 19: Begin state with magnetometer added

I gently move and rotate the phone. After the manipulation, the phone ended up in a posture with a certain offset with the real Google one.

After I place the phone exactly beside my computer, the estimated picture of the phone starts to rotate.

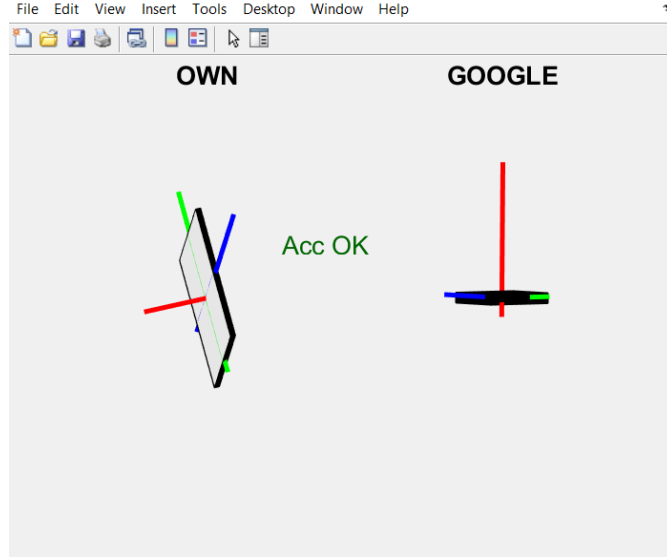


Figure 20: Place the phone beside the computer

When I try to return the phone to the operating point, I observed that our filter cannot return to the true state point, and started to swing around it. That is because in the measurement model, we assume the $f_k^m = 0$, but in reality, this part has a certain value that is attributed to the state q_k , which says our filter now works worse than without using it.

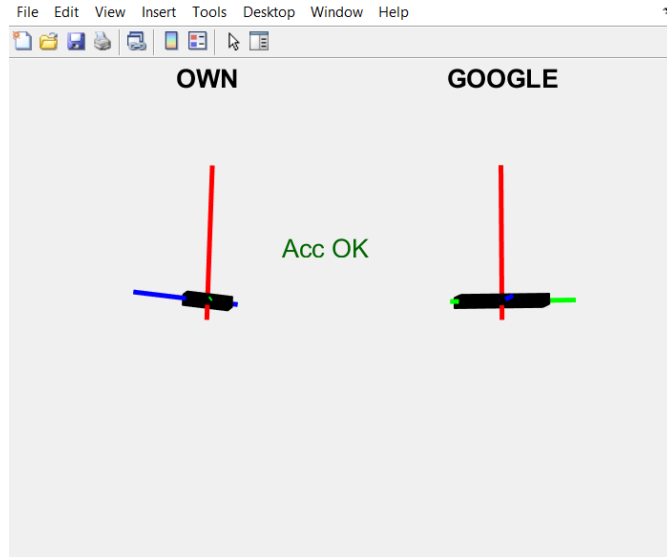


Figure 21: Return to beginning

5.3 Task 11

To construct a basic outlier rejection algorithm, begin by computing the predicted value of $\hat{L}_k = (1 - \alpha)L_{k-1} + \alpha\|m_k\|$. This principle bears a resemblance to a complementary filter.

Then the rejection is set as:

$$\|m_k - \hat{L}_k\| \leq k \cdot \hat{L}_k$$

where $k = 0.1$

This formula implies that the update of the magnetometer is only deemed valid when its measured value falls within a narrow range of 10% around the meticulously predicted value.

When the values of $\alpha = 0.1$ and $L_0 = 0$ are employed, the phone continues to perform a rotational motion.

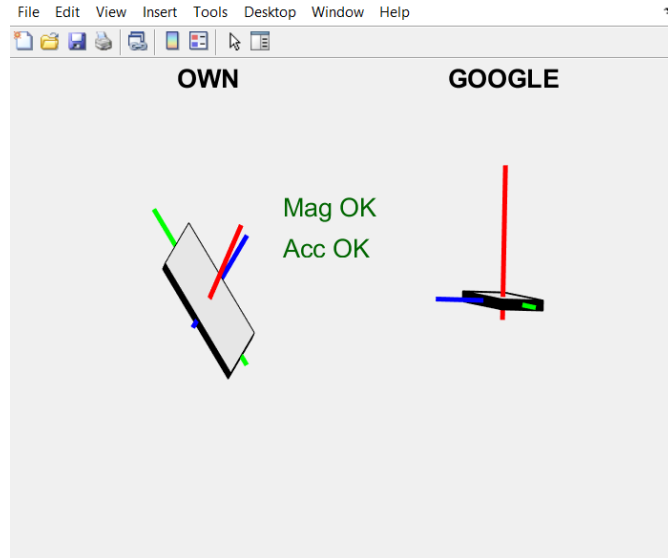


Figure 22: Set $\alpha = 0.01$

When the values of $\alpha = 0.01$ and $L_0 = 0$ are set, the phone is able to return to its true state and partially alleviate the offset caused by inaccuracies in the accelerometer. However, it still exhibits a sway.

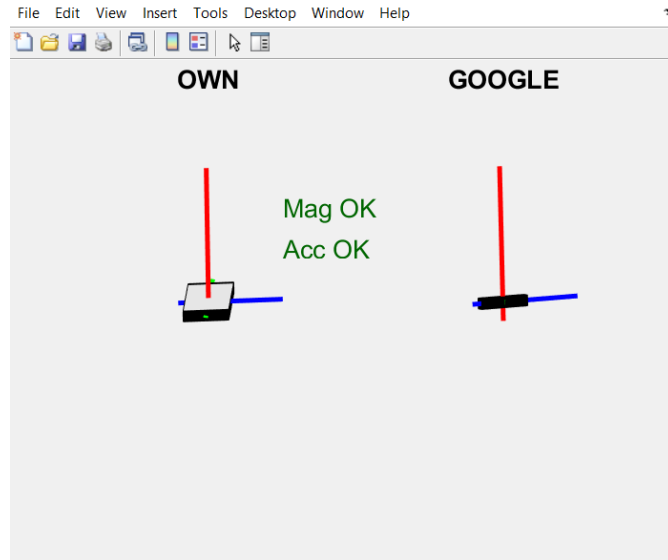


Figure 23: $\alpha = 0.01$

When set $\alpha = 0.001$ and $L_0 = 0$, the result holds.

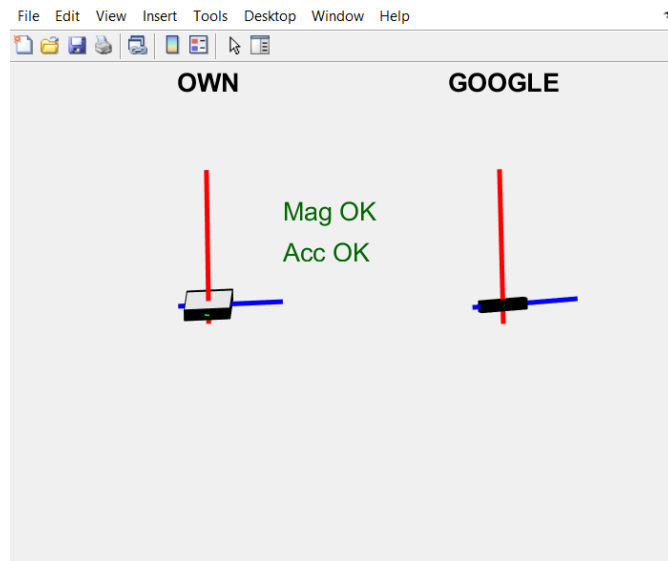


Figure 24: $\alpha = 0.001$

Upon implementing outlier rejection, I observed that when the mobile phone is placed close to a source of interference, specifically my computer, the update

of the magnetic state, or "mag" state, is declined. Thus, it effectively eliminates magnetic field interference during movement.

However, considering the algorithm of the AR filter, it is a filtering algorithm based on the previous moment. As long as the phone maintains a particular posture and position for a brief period, it accepts the current magnetometer reading, whatever it is.

Therefore, the underlying assumption of this algorithm is that the phone experiences a sudden magnetic field disturbance from an environment with overall weak background noise, which eventually disappears after a certain duration. This enables the phone to reject the sudden occurrence of magnetic interference. However, it does not distinguish the continuous constant noise unrelated to the Earth's magnetic field.

Hence, when I placed the phone next to the computer, introducing magnetic field interference to test this theory, I did indeed observe that after a while, it started rotating just like it would without the inclusion of outlier rejection.

6 Task 12

During my verification process, I recalibrated the mean and covariance of each sensor to minimize the artificially introduced errors as much as possible.

For each combination, I introduced three types of motion: primarily focused on rotation around the x-axis, primarily focused on rotation around the y-axis, and primarily focused on rotation around the z-axis.

They will be labeled as 1, 2, and 3 in the plots for each combination.

Before each experiment, sufficient time was given to the phone to initialize and calibrate the biases. This information can be observed from the graphs.

6.1 All sensors

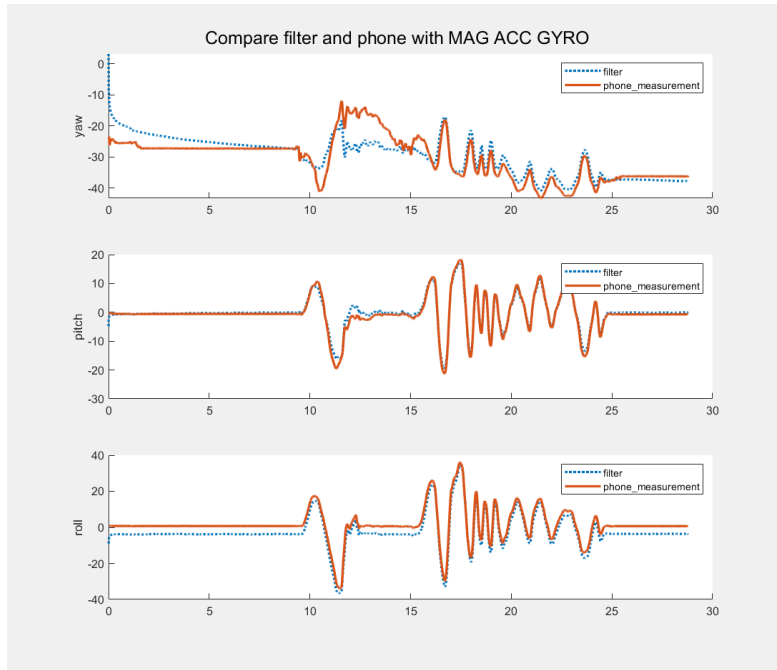


Figure 25: All Sensors: 1

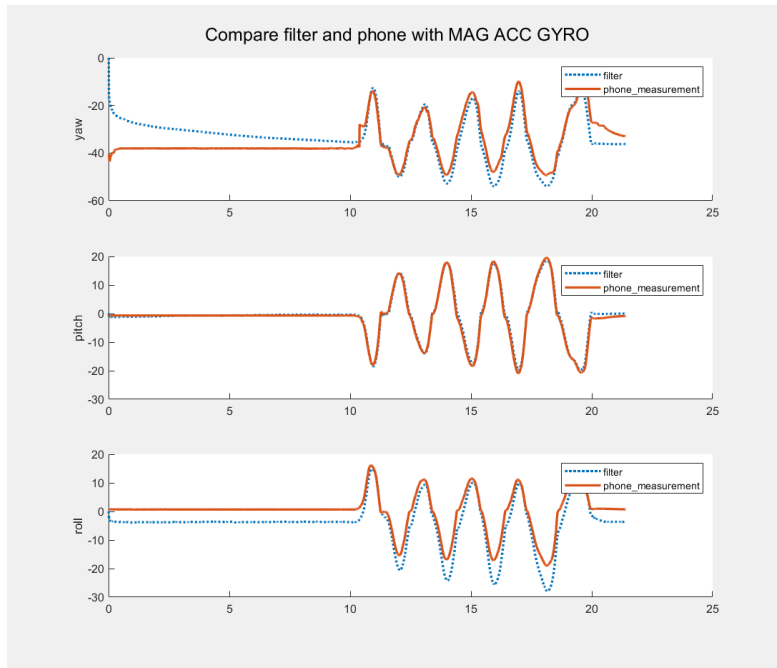


Figure 26: All sensors: 2

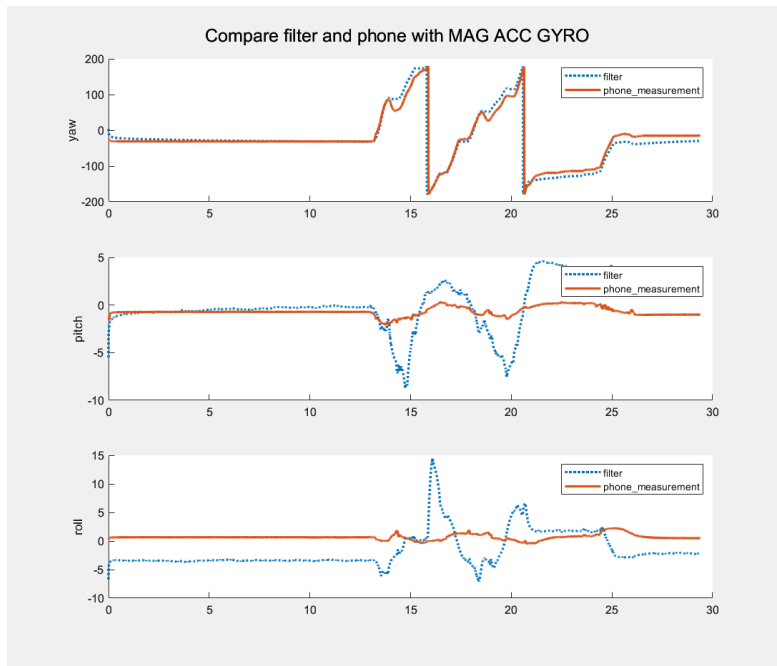


Figure 27: All sensors: 3

From the three experiments, it can be observed that when all the sensors (mag, acc, gyro) are enabled, our designed filter performs relatively well in tracking rotations around the x-axis and y-axis. However, when facing rotations around the z-axis, except for the yaw angle, the tracking performance for the other two angles is very poor.

6.2 Acc and Gyro

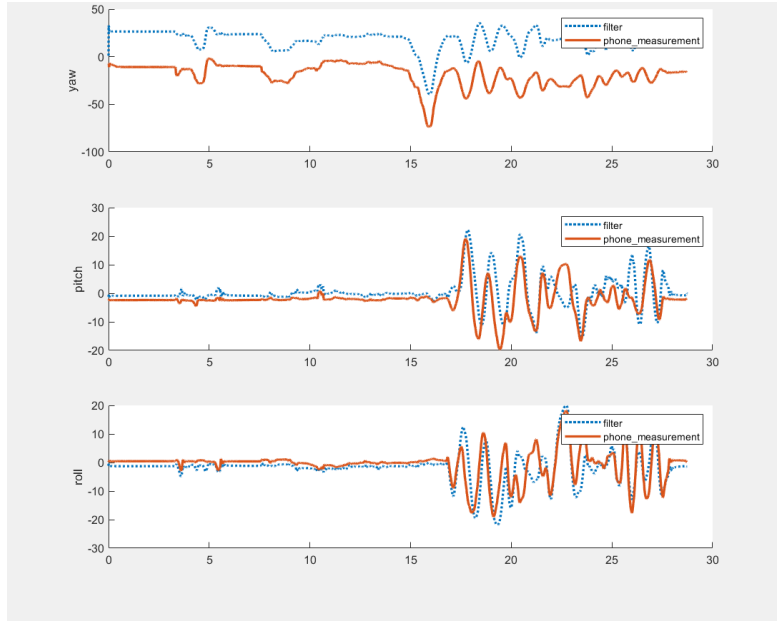


Figure 28: Acc and Gyro : complex

From figure 28, it seems that without the magnetometer, the estimate result works really bad in yaw.

So test the special rotate for yaw:

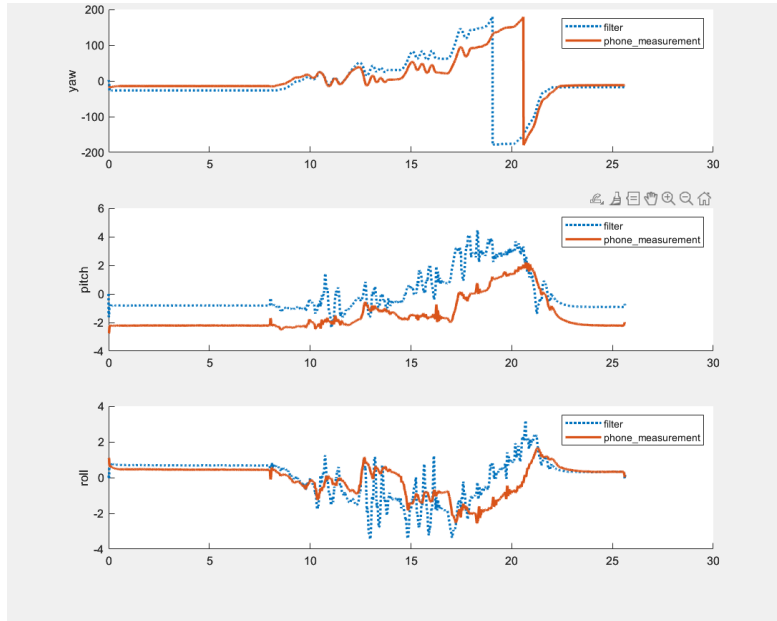


Figure 29: Acc and Gyro : 3

It is difficult to evaluate whether the performance in the current situation is better than having the magnetometer present, since it seems catch more information than previous.

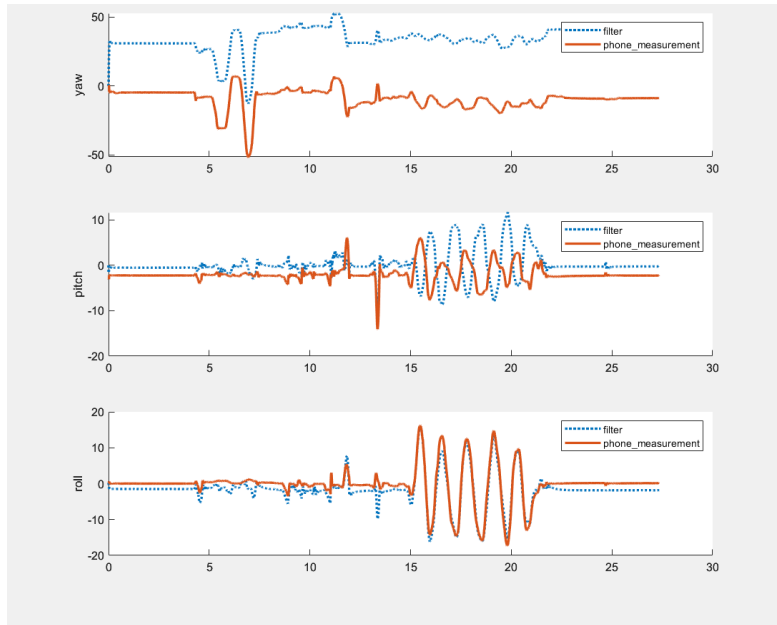


Figure 30: Acc and Gyro : 1

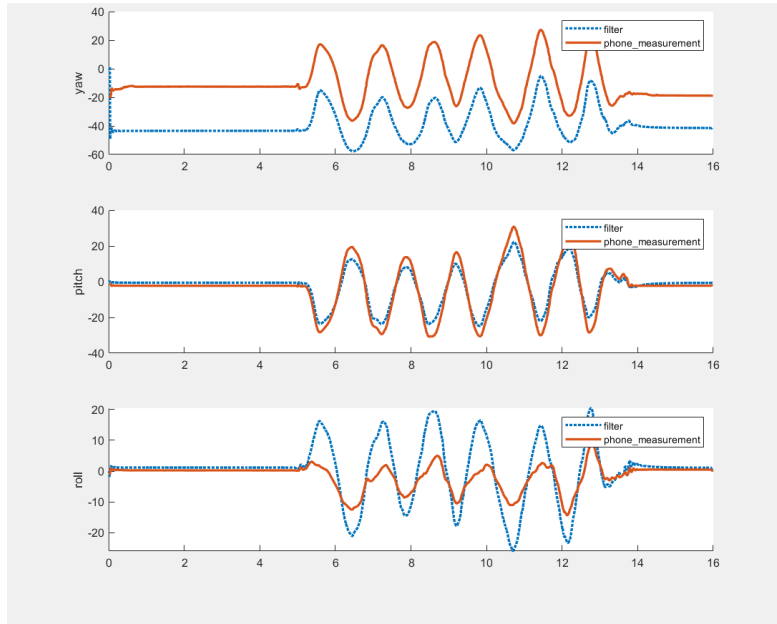


Figure 31: Acc and Gyro : 2

From figure 30 and figure 31, it can be observed that without the magnetometer, the phone has lost its ability to correct its offset in yaw. Additionally, the tracking speed has decreased, and it can only achieve good tracking performance on axes with significant and active changes.

6.3 Acc and Mag

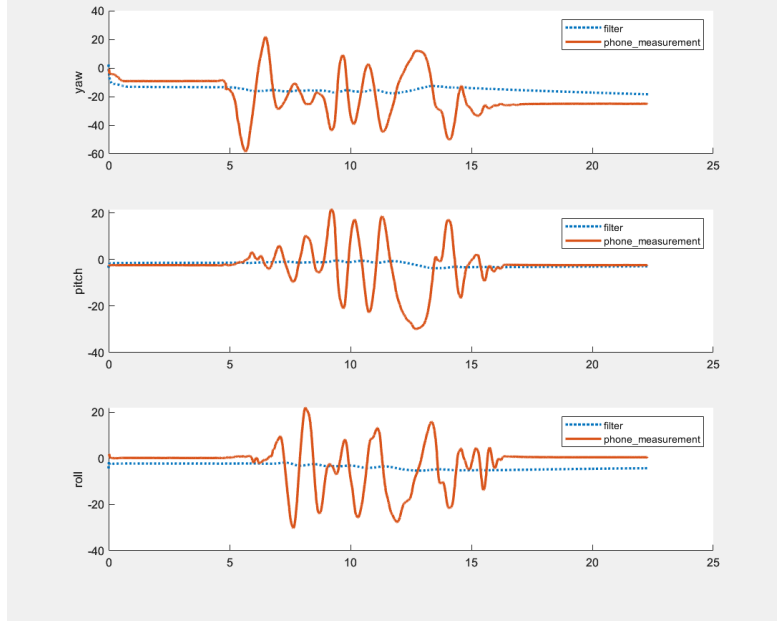


Figure 32: Acc and Mag: complex

It can be observed that without the gyroscope, the filter is unable to function properly.

This is because without the gyroscope, the filter cannot accurately sense the device's rotation, leading to the inability to estimate the attitude. While the magnetometer and accelerometer can provide some information about the device's orientation, their measurement range is limited and susceptible to external interference. Without the angular velocity measurements provided by the gyroscope, the filter cannot effectively fuse and estimate the orientation using these sensor data.

Therefore, without the gyroscope, the filter lacks angular velocity information and is unable to perform accurate attitude estimation, resulting in its inability to function properly and being paralyzed.

6.4 Gyro and Mag

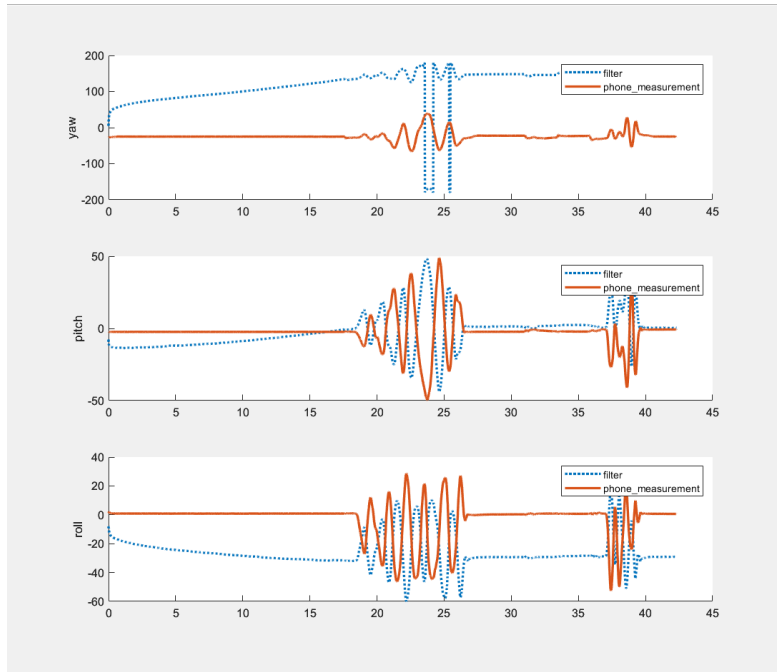


Figure 33: Gyro and Mag: complex

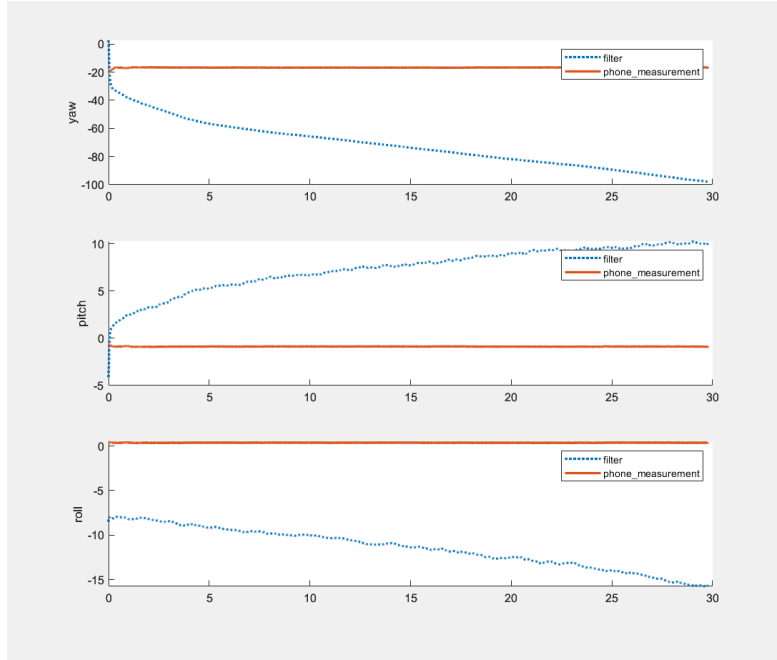


Figure 34: Gyro and Mag: flat

It has been observed that without the accelerometer, the device's attitude experiences continuous drift. This drift is primarily caused by the continuous updates from the magnetometer. Although the gyroscope can accurately perceive angular velocity, its measurements do not have practical significance due to the incorrect orientation of the coordinate axes. As a result, the gyroscope measurements are unable to salvage the performance of the filter.